Developing asymmetries in AGB stars : occurrence, morphology and polarization of circumstellar Masers

Amiri, N.

1 Introduction

1.1 Outline

The aim of the research presented in this thesis is to probe the asymmetries in the circumstellar envelopes of Asymptotic Giant Branch (AGB) and post-AGB stars which will likely evolve into asymmetric Planetary Nebulae (PNe) at the end of their life. I present the observations and modeling of astrophysical masers which occur in the outflows from evolved stars. The masers provide excellent tracers of the outflows at various distances from the central AGB stars. In this introduction I explain the AGB phase which is the last stage of stellar evolution. This is followed by an overview of the asymmetric PNe problem. Then I discuss the circumstellar masers which occur in the outflow from evolved stars. Next, I will explain how we use masers as astronomical tools to probe the magnetic fields and morphology of the outflow in the CSEs. Finally, I will present the main goals and the outline of the chapters of the thesis.

1.2 Asymptotic Giant Branch Phase

After a star leaves the main sequence, it evolves through several evolutionary stages, including the red giant branch, the horizontal branch and the AGB phase (Fig. 1.1). The last phase of the evolution for low to intermediate mass stars (1-8 $M_{\odot}$) is the AGB phase. In this stage, the star is left with a core of carbon and oxygen and two burning layers of Hydrogen and Helium surround the core. More than 90% of the stars including our Sun will evolve into the AGB phase. These stars will become >3000 times more luminous than our Sun. An extensive review of AGB stars is given by Habing (1996).

In the AGB phase the stars lose significant amounts of their mass to the interstellar medium in the form of stellar winds. The outflows form the circumstellar envelopes (CSEs) around the AGB stars (Fig. 1.2). In regular AGB stars, the CSEs are generally thought to be spherically symmetric. However, departures from spherical symmetry likely occurs in the late AGB or early post-AGB stage. AGB stars are known to be variable at visual and infrared wavelengths. Mira variables have periods of 100 days or more.

For a long time, OH/IR stars were thought to represent more evolved AGB stars (e.g. Bedijn 1987), although there is evidence that OH/IR stars come from a distinct higher mass population (e.g. Whitelock et al. 1994, Chen et al. 2001). The CSEs of these stars are denser and larger than those of Mira variables. The average expansion velocity in the CSEs is in the range 5-15 km s^{-1}. The mass loss rate ranges from 10^{-8} to 10^{-4} $M_{\odot}$/yr. Such a high mass loss rate could result in the situation that the central AGB star is highly obscured and therefore the emission radiated from the photosphere at infrared and optical wavelengths will be absorbed by the dust and re-emitted at longer wavelengths. The dust shell constitutes about one percent of the total mass of the CSEs. However, it likely plays a major role in driving the wind through the radiation pressure effect. In this scenario, the dust particles absorb the radiation and gain momentum. The particles transfer the momentum to the gas by friction, which governs the mass loss.

After the mass loss stops in the AGB phase, the star will evolve into the post-AGB and probably PNe phases.

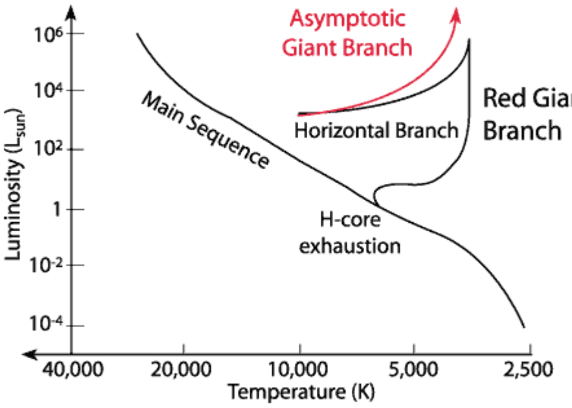

Figure 1.1 – Hertzsprung-Russell Diagram (HRD) which shows the evolutionary track of stars.

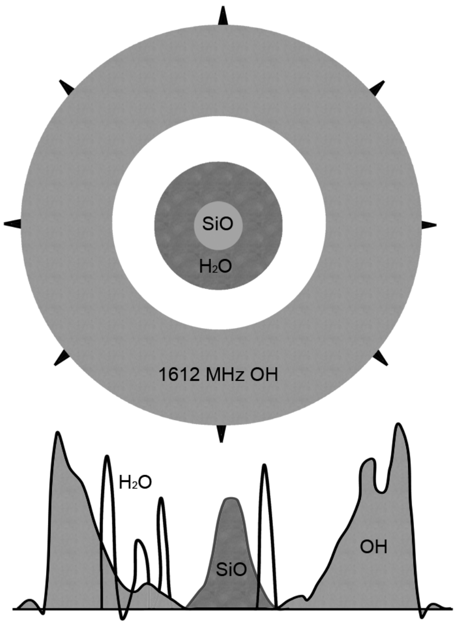

Figure 1.2 – A schematic view of the CSE of a typical oxygen-rich AGB star. SiO masers occur close to the photosphere and show single peak profiles. H_2O masers occur at intermediate distances and exhibit irregular profiles. The 1612 MHz OH masers emit at the outer part of the CSE and display double peak profiles, which corresponds to the front and back side of the shell. Asphericity likely occurs in the late AGB or early post-AGB stage. Credit: Lor*á*nt Sjouwerman.

1.2.1 Planetary Nebulae

After the nuclear burning stops in the H and He burning shells, the central AGB star becomes a hot white dwarf with a surface temperature of ∼30,000 K or more. The remnant CSE ejected previously in the AGB phase becomes a PN where the ultraviolet radiation from the central white dwarf ionizes the gas. The majority of the observed PNe exhibit a range of complex morphologies (e.g. Manchado et al. 2000, Balick et al. 1987), whereas their progenitor AGB stars are generally observed to be spherically symmetric (e.g. Bowers et al. 1983). Fig. 1.3 shows the observed shapes of PNe obtained by the Hubble Space Telescopes (HST). PNe are thought to form as a result of the interaction between the fast post-AGB wind (∼1000 km s^{-1}) and an asymmetric dense and cool AGB wind (e.g. Kwok et al. 1978, Balick et al. 1987). HST imaging of a sample of proto-PNe candidates has shown a wide variety of morphologies including bipolar structures (Sahai et al. 2007). Collimated outflows which operate in the early proto-PNe stage have been proposed as responsible agents for the formation of bipolar PNe (Sahai & Trauger 1998). The mechanisms for producing fast and collimated outflows could result from the presence of a binary companion (e.g. Morris 1987). Alternatively, theoretical models by García-Segura et al. (2005) show that magnetic fields could have an important role in collimating the jets.

The a-spherical shapes of PNe could indicate that departure from spherical symmetry occurs during the transition from the AGB phase to the PNe stage, the so called proto-PNe phase. Therefore, probing asymmetries even in the earlier stage represented by the CSEs of AGB stars is essential to understand the origin of complex morphologies observed in PNe. The CSEs of AGB stars harbor molecular and atomic species as well as the dust.

1.3 Circumstellar Envelopes

The main tracers of the properties of the CSEs are the atomic and molecular lines ranging from the cm to μm wavelength (radio to infrared), as well as sub-mm to infrared continuum and spectral features of the dust. In particular the CSEs harbor various *maser* species at different distances from the central stars:

1.3.1 What is a Maser?

Maser stands for microwave amplification by stimulated emission of radiation. The essential property of a maser transition is the population inversion, where the population of the upper energy level is higher than the lower level population. A Laser is the equivalent of a Maser, which occurs at higher frequencies in the ultraviolet or visible region of the electromagnetic spectrum.

The fundamental physical mechanism for maser emission is stimulated emission which was first introduced by Einstein in 1917. Fig. 1.4 shows the principle of maser emission schematically. Masers occur naturally in space and different molecular species can exhibit maser emission. This implies that there are regions in space, in which the physical

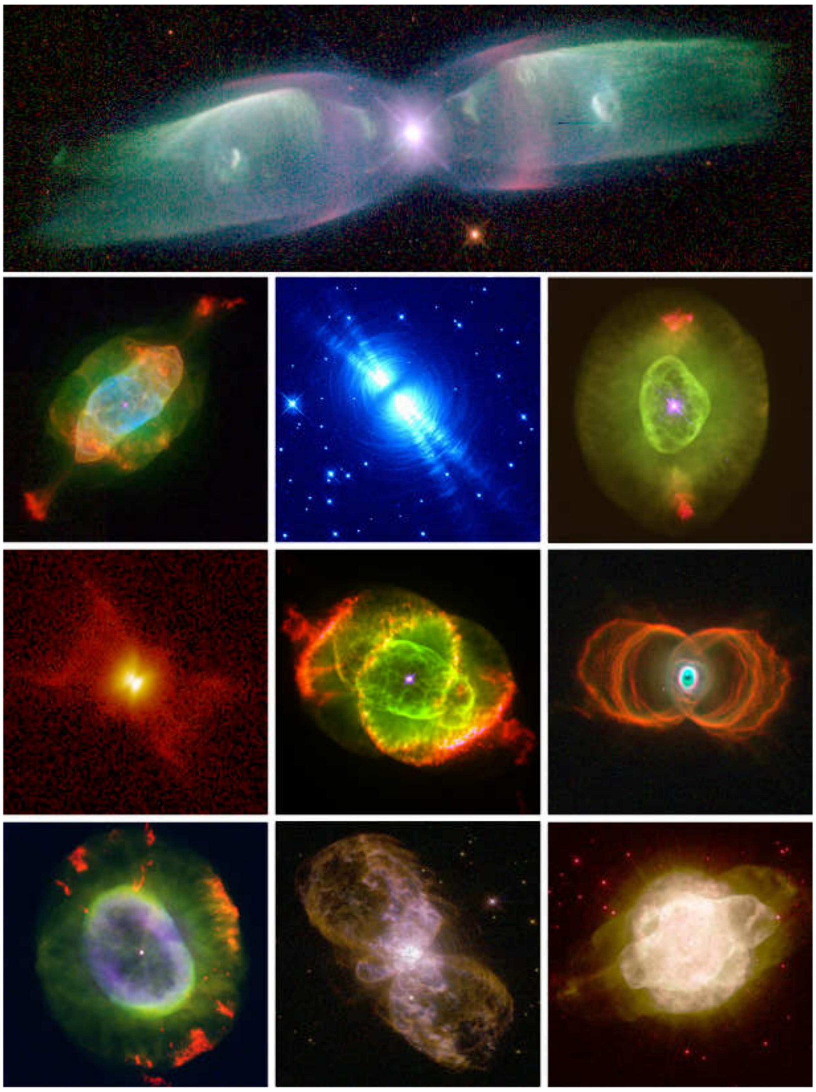

Figure 1.3 – A montage of Planetary Nebulae observed with the Hubble Space Telescope. Credit: NASA-Bruce Balick.

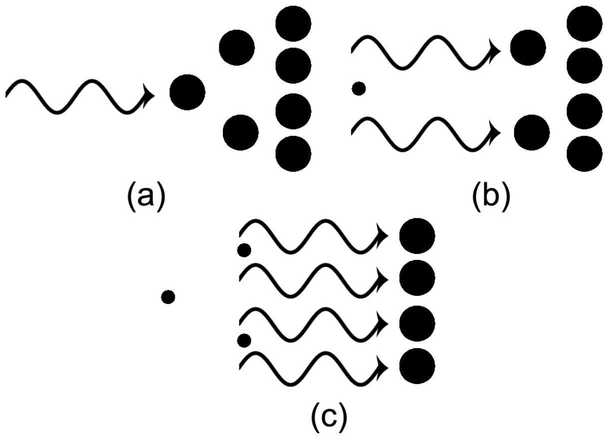

Figure 1.4 – Principle of maser emission: In all frames, the large circles show molecules excited to the upper energy state by a pump. The small circles indicate the molecules in the low energy state. 'a' panel: the molecule in the excited energy state is stimulated by a photon of wavelength λ. 'b' panel: The molecule absorbs the photon and re-emits two photons instead to return to the low energy state. These two photons hit the next two excited molecules, which results in 4 photons (panel 'c'). This process continues and as the radiation propagates through the medium, the maser amplifies the radiation exponentially at wavelength λ, as long as it is unsaturated.

conditions are such that deviations from local thermodynamic equilibrium (LTE) are common. For the population inversion to occur, a pumping mechanism is required. Typical pumping mechanisms for astronomical masers include infrared radiation or collision with other molecules. The other necessary condition for masers is velocity coherence along the amplification path. This implies that the radiation is not amplified if the velocity gradient along the amplification path is higher than the thermal line width.

In the CSEs of oxygen-rich AGB stars, three maser species are common: SiO, H_2O and OH masers. The SiO masers occur in the near circumstellar environment in a region between the stellar photosphere and the dust formation zone. The H_2O and OH masers are found progressively at further distances. Fig. 1.2 displays a schematic view of the locations and spectra of maser species in the CSEs. Below, we describe the properties of each maser species. A detailed description of the masers is presented by Elitzur (1992).

1.3.1.1 OH Masers

The OH masers occur at the outer part of the CSEs at distances between 100-10000 AU from the central AGB star. The typical brightness temperature of the masers is in the range $10^8 - 10^{10}$ K. The masers are predominantly observed in the rotational ground level which has the highest population. The ground level transition is split into 2×2 levels by Λ-doubling and hyperfine interaction (Fig. 1.5, Wilson et al. 1990). The masers are observed at both satellite line (1612 MHz) as well as the main line (1667 and 1665 MHz) transitions. The pumping mechanism for the 1612 MHz transition is known to be due to the infrared dust radiation at 35μ and 53μ. However, the pumping of the main line transitions is more complex.

As shown in Fig. 1.2, the OH masers are emitted from the outer part of oxygen-rich CSEs, in a region where the photodissociation of the H_2O molecules produces OH. At these distances the gas has reached the terminal velocity and therefore the velocity coherent path length is longest along the radial direction. The observed properties of the main line transitions are somewhat different from the satellite lines, which could imply a different physical mechanism and location of the masers in the CSEs. The 1612 MHz OH masers exhibit a double peak profile separated by 20-50 km s^{-1}. This characteristic profile can be explained by an expanding shell where there is no radial acceleration. The blue- and red-shifted peaks correspond to the emission from the front and back side of the shell. The expansion velocity is half the velocity separation between the two peaks and the middle point between the two peaks corresponds to the stellar velocity.

1.3.1.2 H_2O Masers

The $(6_{16} - 5_{23})$ H_2O maser transition occurs at 22.23508 GHz. The occurrence of H_2O masers is common in the CSEs of evolved stars. The observed brightness temperature of the masers is in the range $10^{11} - 10^{12}$ K. The pumping mechanism for the masers is thought to stem from collisions with other molecules.

The H_2O masers occur at intermediate distances from the central stars at distances between 5-100 AU from the photosphere. This is a region which experiences significant radial acceleration. Unlike the double peak profile commonly observed for the 1612 MHz OH masers, the H_2O masers do not show regular spectral patterns. In Mira variables the masers usually show emission close to the stellar velocity due to tangential beaming from rapidly accelerating winds (e.g. Chapman & Cohen 1985). However, in higher mass loss OH/IR stars the masers usually exhibit double peak profiles. This could indicate that the masers occur somewhat at further distances from the central star where the masers are mostly radially amplified (e.g. Engels & Lewis 1996).

1.3.1.3 SiO Masers

SiO masers occur in a region between the stellar photosphere and the dust formation zone at distances of 5-10 AU from the central AGB star. Therefore, the masers are excellent tracers of the kinematics and dynamics in regions close to the central star. The SiO molecule exhibits a range of maser spectral profiles; vibrational energy levels up to v=3 and rotational transitions as high as J=8-7 are reported for the masers (e.g. Jewell et al. 1987, Cernicharo et al. 1993, Humphreys et al. 1997). In particular the v=1, J=1→0 and v=1, J=2→1 transitions are known to be more prevalent in the CSEs.

The masers show complex profile structures which spread over a velocity range of ~10-15 km s^{-1} around the stellar velocity. The observed profiles of the masers indicate significant variability in profile shape and brightness temperature. The variability of the

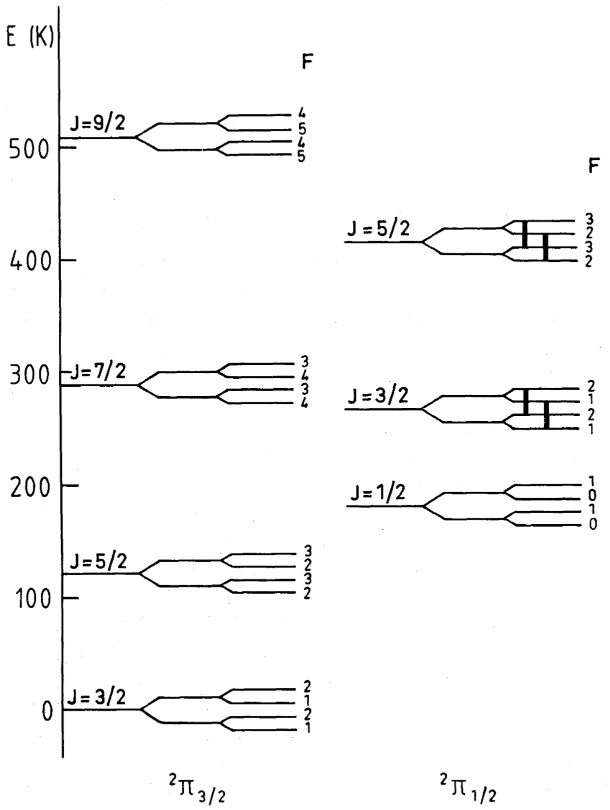

Figure 1.5 – The rotational levels of the OH molecule within 500 K of the ground state (Wilson et al. 1990). The Λ doubling and hyperfine splitting cause each rotational energy level to split into four groups of lines.

masers is thought to be related to the pulsation of the central AGB star. The typical brightness temperature of the masers is in the range 10^9-10^{10} K. The masers are confined in compact, high brightness spots and Very Long Baseline Interferometry observations around Mira variables reveal ring shape morphologies (Cotton et al. 2008, 2006, Diamond et al. 1994).

1.4 Masers as Tools to Probe the Stellar Evolution

The circumstellar masers which occur in the CSEs of evolved stars are useful tracers of the outflow at various distances from the central AGB stars. The masers exhibit very high brightness temperatures ($\sim 10^9$ K or higher), providing spectacular targets for interferometry and in particular for Very Long Baseline Interferometry (VLBI) observations. In my research I used various interferometer arrays including the European VLBI Network (EVN), the Very Long Baseline Array (VLBA), the Expanded Very Large Array (E-VLA) and the UK Multi-Element Radio Linked Interferometer Network (MERLIN) to map the circumstellar masers up to 0.5 mas resolution. Additionally, we performed single dish observations of the circumstellar masers using the radio telescopes including the Effelsberg Telescope and the Green Bank Telescope (GBT). Below, I explain the main goals of performing these observations:

1.4.1 Morphology of the CSEs

Interferometric observations of the masers enable us to obtain the spatial distribution of the masers in different regions of the CSEs in AGB and post-AGB stars. This helps us to study the asymmetries that already start in the AGB/ post-AGB phase which will evolve into a-spherical PNe. Furthermore, high resolution maps of maser spots enable us to compare the maser emission mechanism in different classes of evolved stars including Mira variables and higher mass loss OH/IR stars and in particular to understand how the distribution of the masers changes as the stars evolve through the AGB phase.

In particular, a class of proto-PNe candidates have been discovered, which exhibit high velocity H_2O maser jets ($\sim$200 km s^{-1} or more), much larger than the OH maser velocity extent (Likkel et al. 1992). VLBI observations of the H_2O masers of the so-called water fountain sources have shown collimated H_2O maser outflows (e.g. Imai et al. 2002, Boboltz & Marvel 2005). The observed spatial distribution and spectral characteristics of this class of sources is not consistent with those of regular AGB stars. An archetype of this class of objects is W43A. Fig. 1.6 displays the elongated dust emission of this star at 12.8 μm obtained with the Very Large Telescope (VLT) spectrometer and imager for the mid–infrared (VISIR, Lagadec et al. 2011). Overlaid are the H_2O and OH maser features obtained from high resolution interferometric observations. The dust image is clearly elongated in the direction of the H_2O maser jet. This could indicate that during the post-AGB phase the jets carve out the CSEs and leave an imprint which manifests itself as asymmetric PNe at the later stage in the evolution. This implies that other regions of the CSEs of these objects (e.g. OH and SiO maser regions), may also show deviation

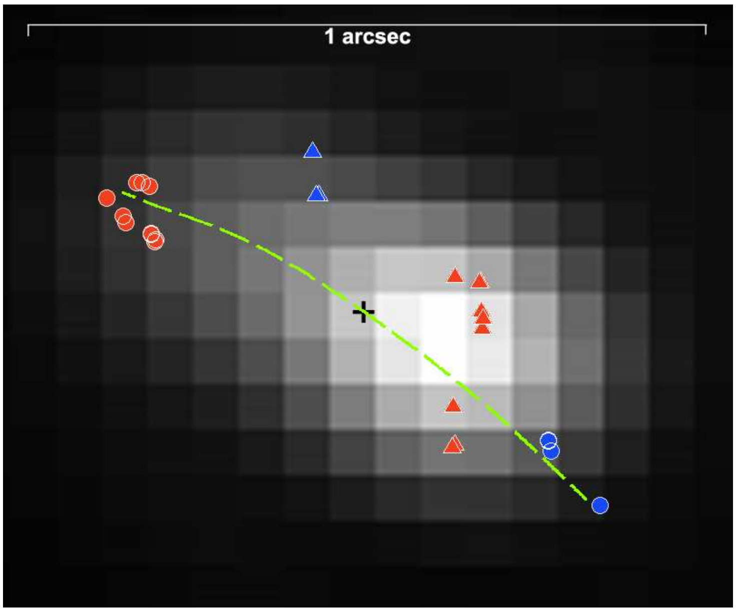

Figure 1.6 – The 12.8 μm dust image of W43A obtained with the Very Large Telescope (VLT) spectrometer and imager for the mid–infrared (VISIR, Lagadec et al. 2011). The overlaid circles and triangles show the H_2O and OH maser features of this star. The dashed line shows the direction of the precessing H_2O maser jet.

from spherical expansion. Therefore, studying the CSEs of this class of objects using high resolution observations of other maser species at different distances from the central AGB star is essential to understand the evolution of asymmetries as the star climbs the AGB phase.

1.4.2 Polarization of Masers

Polarimetric observations of masers are the best probes of magnetic fields in the CSEs, which enable us to understand the role of the magnetic fields in shaping the CSEs throughout the AGB evolution. The Zeeman splitting measurement of maser species is the most direct way to determine the magnetic field strength and morphology in the CSEs. In the presence of an external magnetic field, the energy levels of the maser transition are split into 2L+1 magnetic sub-levels, where L is the orbital angular momentum quantum number (Fig. 1.7). This implies that the ground state does not split in the magnetic field. The measured Zeeman splitting is related to the molecular structure, the strength of the magnetic field and the angle between the line of sight through the maser and the direction of the magnetic field. While single dish polarimetric observations can in principle only yield the overall field strength and morphology, polarimetric interferometry observations

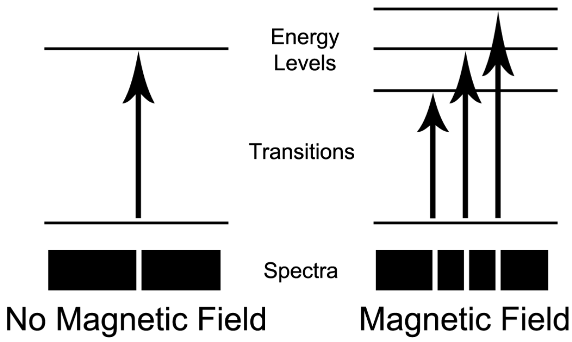

Figure 1.7 – Zeeman effect. In the presence of an external magnetic field, each spectral line is split into 2L+1 sub-levels, where L is the orbital angular momentum quantum number. Therefore, the ground state does not split in the magnetic field.

of circumstellar masers enable us to determine the field strength and morphology for the individual maser features.

Such circular polarization observations revealed significant field strengths in the CSEs. The observations of SiO masers have revealed a field strength of ~3.5 G for a sample of evolved stars (e.g. Herpin et al. 2006). The observed field for OH and H_2O masers is in the range 0.1-10 mG and 0.2-4 G, respectively (e.g Etoka & Diamond 2004, Vlemmings et al. 2002, 2005). Fig. 1.8 displays the magnetic field strength in different regions of the CSEs probed by maser polarization measurements. The figure shows that there is a clear relation between the field strength and the distance from the central star.

Additionally, the linear polarization measurements of the masers can probe the direction of the magnetic field projected on the plane of the sky. For regular masers in the CSEs, SiO masers typically exhibit high fractional linear polarization up to 100%. OH masers show polarization fractions up to tens of percent. However, H_2O maser observations do not indicate significant linear polarization.

The polarization analysis of the circumstellar masers is somewhat complex and alternative effects have been introduced which prohibit one to interpret the observed polarization as a measure of the magnetic field strength and morphology. The maser radiative transport can introduce preferred asymmetries not necessarily due to the magnetic effects. Therefore, this requires careful consideration of non-Zeeman mechanisms in order to reliably measure the magnetic fields. For OH and H_2O masers the non-Zeeman effects are not significant (Amiri et al. 2010, Vlemmings et al. 2005), while in the case of SiO masers it is not possible to distinguish between the Zeeman and non-Zeeman mechanisms.

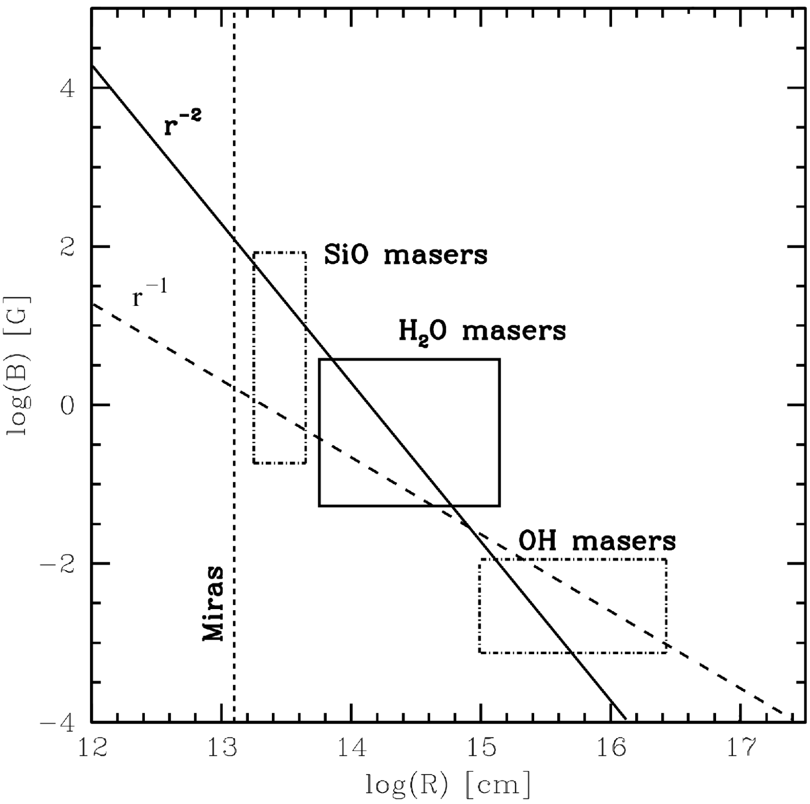

Figure 1.8 – The magnetic field strength (B) as a function of distance, R, from the center of the star. The boxes indicate the observed field strength obtained from polarimetric measurements of masers. The thick solid and dashed lines display an r^{-2} solar-type and r^{-1} toroidal magnetic field morphology. The vertical dashed line shows the stellar surface (Vlemmings et al. 2005).

1.4.3 Variability of the Masers

The circumstellar masers, in particular H_2O and SiO masers, are known to be variable in flux density and spectral profile. The lifetime of the individual maser features is a few months to years and the flux density may vary by as much as 2 orders of magnitude. The variability of the masers is thought to be related to the stellar pulsation as well as the changes in physical conditions in the environment in which masers occur. For example, H_2O masers are located in a region where shock waves driven by stellar pulsation are propagating through the H_2O maser zone (Rudnitskii & Chuprikov 1990, Shintani et al. 2008).

By single dish monitoring observations of the masers, we can study the variability statistics of the masers. This helps us to understand how rapidly the physical conditions in the CSEs change in time. Some masers show decrease in flux density and it is not clear however, if the masers that show deviation and in particular a decline in flux density, continuously lose flux until they fade away, or they rise up again.

1.5 This Thesis

The research in this thesis is focused on observations of masers around evolved stars. The observations include the use of radio interferometers as well as single dish telescopes. The aim of the the research is to address several key questions:

1. What is the role of the magnetic field in shaping the circumstellar environment of AGB stars?

2. Are strong magnetic fields common in different classes of AGB stars?

3. Is the occurrence of a-spherical morphologies common in the CSEs of evolved stars?

4. Are water fountain sources commonly found among post-AGB candidates?

In this thesis, Chapters 2, 3, 4 and 6 address questions 1, 2 and, while Chapter 5 focuses on question 4.

1.5.1 Outline of the Thesis & Main Results

- *Chapter 2&3*

  In chapters 2&3, we present the OH maser polarimetric observations of three water fountain sources (W43A, OH 12.8-0.9 and OH 37.1-0.8) with the UK MERLIN interferometer. The main goal of the observations is to understand whether large scale magnetic fields exist in the circumstellar environment of these stars.

  In Chapter 2, we report an average magnetic field of 100 μG measured for the OH maser region of W43A. Additionally, we present the polarimetric observations of the H_2O maser jet of this star with the Green Bank Telescope. From the observations we measured a magnetic field of 30 mG for the red-shifted lobe of the H_2O maser jet. Interestingly, we found that the measured field for the OH masers of W43A is consistent with that extrapolated from the H_2O maser measurements. Therefore, our measurements show that the magnetic fields likely play an important role in shaping the entire circumstellar environment of this star.

In Chapter 3, for the first time, we present the spatial distribution of the OH maser features of OH 12.8-0.9 and OH 37.1-0.8. We found that the OH maser of both sources shows signs of a-spherical expansion. Additionally, we performed kinematical re-construction of the masers assuming a uniform distribution in the CSEs. The aim is to understand the distribution of the OH masers in water fountain sources with respect to the H_2O maser jet. In this class of objects, the jet-like outflows transform the spherically symmetric CSEs into a-spherical morphologies. We developed software which calculates the velocity coherent path length along the line of sight. Comparison of the OH maser observations (spectral profile and spatial distribution) with the reconstruction results shows that the OH masers of W43A are likely located in the equatorial region of the outflow, whereas for OH 12.8-0.9 the OH masers are likely located in a biconical outflow surrounding the H_2O maser jet. Additionally, we found that the H_2O maser jet of this star is located inside the OH maser shell. This could indicate that this source is still in the AGB phase and the jet has recently launched in this star.

- *Chapter 4*

  In Chapter 4, we present H_2O maser polarimetric observations of a sample of evolved stars. While previous measurements show significant field strength in Mira variables, it is not clear whether the occurrence of such strong magnetic fields is common in different classes of AGB stars. We observed three Mira variables and three higher mass loss OH/IR stars with the Green Bank Telescope. Even though the measured field strength is underestimated in single dish measurements due to the spectral blending, the observations measure the overall field strength in stars which are not strong enough for VLBI observations.

  From the observations we measured a magnetic field of 18.9±3.8 mG for the H_2O maser region of the OH/IR star IRAS 19422+3506, and for the rest of the sources in the sample we only place upper limits on the magnetic field in the range 10-800 mG. Interestingly, we observe a striking double peak profile with emission close to the stellar velocity, which could indicate the presence of a bipolar outflow in this star, as previously observed in water fountain sources.

- *Chapter 5*

  In Chapter 5, we present multi-epoch observations of the H_2O masers of a sample of post-AGB candidates with the Effelsberg telescope. The aim of the observations was mainly to identify more water fountain sources to create a statistically significant sample of these important transition objects. We found six water fountain candidates with striking double peak profiles which could hint that the masers are occurring in bipolar outflows. Follow up high resolution observations are essential to clarify this.

Additionally, multi-epoch observations enabled us to study the variability statistics and the change in the profile structure of the masers. We found that for a large number of sources the masers show significant deviation in flux density up to an order of magnitude. This could imply significant change in the physical conditions of the circumstellar environment. Furthermore, we found that ten sources which were detected in single dish observations 20 years ago (Engels & Lewis 1996), have now disappeared in our multi-epoch observations. This could imply a limited lifetime of the masers in the AGB phase (~60 years). Additionally, the statistical analysis indicate good correlation between the stellar pulsation and the H_2O maser variability.

Furthermore, we detected the H_2O masers of the supposedly dead OH/IR star IRAS 18455+0448. This object is considered as a prototype of a dead OH/IR star after the rapid disappearance of the 1612 MHz OH masers (Lewis et al. 2001). We performed follow up OH maser observations of this star at 1612, 1665, 1667 MHz. The observations showed that the 1612 MHz OH masers have not reappeared together with the H_2O masers, and importantly, that the 1665 and 1667 MHz OH masers have now also decreased dramatically in strength.

- *Chapter 6*

In Chapter 6, we present the first SiO maser map of an OH/IR star at high angular resolution. We observed the v=1, J=1→0 transition of the SiO masers of OH 44.8-2.3 with the VLBA. The observations show a circular ring pattern at a radius of 5.4 AU from the photosphere, assuming a distance of 1.13 kpc previously measured using the phase lag method. Furthermore, we found that the SiO masers of this star are located at ~1.9 stellar radii which is similar to the location of SiO masers in Mira variables.

The observations show that the SiO maser features of OH 44.8-2.3 show significant linear polarization up to 100%. While the linear polarization vectors are consistent with a dipole field morphology, we can not rule out other complex field morphologies including toroidal or solar type fields. Additionally, the circular polarization analysis shows a tentative detection of circular polarization at ~0.7% for the brightest maser feature in the modest spectral resolution data set. Due to the increased noise we can not confirm the detection in the high spectral resolution data set. The measured circular polarization corresponds to a magnetic field of 1.5±0.3 G.

Additionally, we processed the 1612 MHz OH maser observations of OH 44.8-2.3 from the VLA archive. The OH masers exhibit an elongated morphology in the direction where there is a gap in the SiO maser emission. However, the OH masers occur at much larger distance (~1471 AU) from the photosphere than the SiO masers (~5.4 AU). Therefore, it is not clear whether both asymmetries are related. Assuming they are, this shows that there is a global mechanism which modifies the CSEs on many scales. Furthermore, according to the polarization theory for SiO masers, the direction of the magnetic field is either parallel or perpendicular to the preferred direction of the outflow. This could indicate the possible role of the magnetic field in shaping the circumstellar environment of this object.

1.5.2 Conclusions and Outlook

The results presented in this thesis have shown that observations of astrophysical masers at high angular resolution provide a unique tool to study the morphology of the CSEs in different classes of AGB stars. This helped us to better understand the evolution of asymmetries in the CSEs throughout the AGB phase. Our observations have shown that asymmetries can occur in different classes of evolved stars. In particular, polarimetric observations of the masers provide the most direct method to determine the magnetic field strength and morphology at various distances from the central evolved stars. The polarization studies presented in this thesis show that magnetic fields could have a significant role in shaping the circumstellar environment.

Despite the significant progress in the field, a number of crucial questions remained to be answered. For example, the upgraded instruments (EVLA and eMERLIN) will provide the unique opportunity to obtain the position of maser features with respect to the central star more accurately. Together with polarization measurements, this helps us to determine the magnetic field strength and morphology of the CSEs throughout the AGB evolution.

Furthermore, the Atacama Large Millimeter Array (ALMA) will provide an unprecedented sensitivity and angular resolution to study the circumstellar environment of evolved stars in the sub-millimeter regime. Observations of the cold dust and in particular the polarimetric observations enable us to study the morphology and magnetic fields. Additionally, ALMA will open up new horizons to perform high resolution observations of high frequency maser lines for various maser species and in particular high angular resolution and polarimetric observations of HCN and SiS masers in carbon-rich AGB stars.